Magnetocaloric effect of gadolinium in high magnetic fields

T. Gottschall, M. D. Kuz'min, K. P. Skokov, Y. Skourski, M. Fries, O. Gutfleisch, M. Ghorbani Zavareh, D. L. Schlagel, Y. Mudryk, V. Pecharsky, and J. Wosnitza

Phys. Rev. B **99**, 134429 — Published 19 April 2019

DOI: 10.1103/PhysRevB.99.134429

Magnetocaloric effect of gadolinium in high magnetic fields

T. Gottschall,[1,*] M. D. Kuz'min,[2] K. P. Skokov,[3] Y. Skourski,[1] M. Fries,[3] O. Gutfleisch,[3] M. Ghorbani Zavareh,[1] D. L. Schlagel,[4] Y. Mudryk,[4] V. Pecharsky,[4,5] and J. Wosnitza[1,6]

[1] *Dresden High Magnetic Field Laboratory (HLD-EMFL), Helmholtz-Zentrum Dresden-Rossendorf, 01328 Dresden, Germany*
[2] *Aix-Marseille Université, IM2NP, UMR CNRS 7334, F-13397 Marseille Cedex 20, France*
[3] *Technische Universität Darmstadt, Institut für Materialwissenschaft, 64287 Darmstadt, Germany*
[4] *Ames Laboratory, U.S. Department of Energy, Iowa State University, Ames, IA 50011-3020, U.S.A.*
[5] *Department of Materials Science and Engineering, Iowa State University, Ames, IA 50011-2300, U.S.A.*
[6] *Festkörper- und Materialphysik, TU Dresden, 01062 Dresden, Germany*

(Dated: April 8, 2019)

The magnetocaloric effect of gadolinium has been measured directly in pulsed magnetic fields up to 62 T. The maximum observed adiabatic temperature change is $\Delta T_{\rm ad} = 60.5$ K, the initial temperature T_0 being just above 300 K. The field dependence of $\Delta T_{\rm ad}$ is found to follow the usual $H^{2/3}$ law, with a small correction in $H^{4/3}$. However, as H is increased, a radical change is observed in the dependence of $\Delta T_{\rm ad}$ on T_0, at $H = $ const. The familiar caret-shaped peak situated at $T_0 = T_{\rm C}$ becomes distinctly asymmetric, its high-temperature slope becoming more gentle and evolving into a broad plateau. For yet higher magnetic fields, $\mu_0 H \gtrsim 140$ T, calculations predict a complete disappearance of the maximum near $T_{\rm C}$ and an emergence of a new very broad maximum far above $T_{\rm C}$.

I. INTRODUCTION

The study of the magnetocaloric effect (MCE) in very high magnetic fields is primarily of fundamental interest. A key quantity describing the MCE is the adiabatic temperature change, $\Delta T_{\rm ad} = T - T_0$, determined under standard conditions: the initial state is at zero magnetic field and temperature T_0; the final state is at $H \neq 0$ and temperature T. The MCE is usually presented graphically as $\Delta T_{\rm ad}$ versus T_0 for constant H. For a conventional ferromagnet when the MCE is measured in low fields ($\mu_0 H \lesssim 10$ T) a plot of $\Delta T_{\rm ad}$ as a function of T_0 has a characteristic *caret*-like shape[1,2], with a sharp and nearly symmetric peak at the Curie temperature, $T_{\rm C}$. We call a ferromagnet conventional if the phase transition at the Curie point is of second order; an archetypal example is gadolinium which is amongst the most important magnetocaloric materials for room temperature application.

Yet, a simple physical argument shows that for large H, the shape of the $\Delta T_{\rm ad}$-vs-T_0 graphs should be quite different from that known from low-field studies. Namely, there should be no maximum at $T_0 = T_{\rm C}$. This prediction is known[3], but little appreciated. The demonstration is easier for $H \to \infty$. The increment of entropy is presented as a sum of lattice and magnetic terms,

$$dS = \frac{3Nk_{\rm B}}{T}dT + dS_M \qquad (1)$$

where N is the total number of atoms and $k_{\rm B}$ the Boltzmann constant. The temperature is assumed to be slightly above $T_{\rm C}$ and well-above the system's Debye temperature, $T_{\rm D}$. Consequently, the first term is derived from the Dulong-Petit value of the lattice specific heat $3Nk_{\rm B}$. This is a realistic assumption for Gd, having $T_{\rm C} = 294$ K and $T_{\rm D} = 184$ K[4].

We now consider an adiabatic magnetization process whose initial state is fully demagnetized and characterized by $S_M = N_M k_{\rm B} \ln(2J+1)$, where N_M is the number of "magnetic" atoms in the system and J is their total angular momentum (we assume localized $4f$ electrons and neglect the contribution of the conduction electrons for simplicity here). The final state is magnetized to saturation, with $S_M = 0$. For such a process Eq. (1) becomes

$$0 = 3Nk_{\rm B} \ln\left(\frac{T}{T_0}\right) - N_M k_{\rm B} \ln(2J+1). \qquad (2)$$

Hence, the temperature for $H \to \infty$ is expressed as follows[3]:

$$T = (2J+1)^{N_M/3N} T_0. \qquad (3)$$

For Gd ($N_M = N$ and $J = 7/2$), this simplifies to

$$T = 2T_0 \qquad (4)$$

and the adiabatic temperature change is given by

$$\Delta T_{\rm ad} = T_0. \qquad (5)$$

Thus, for $H \to \infty$ and $T_0 > T_{\rm C}$, $\Delta T_{\rm ad}$ should increase with T_0 with a proportionality factor of 1 for Gd. The slope, known to be negative above $T_{\rm C}$ for small H ($\mu_0 H \lesssim 10$ T), should therefore change sign and become positive at a certain critical value of H, so that the maximum of $\Delta T_{\rm ad}$ at $T_0 = T_{\rm C}$ should disappear.

For $T_0 < T_{\rm C}$, $\Delta T_{\rm ad}$ is always a growing function of T_0, whatever the value of H. In general, the description is more complicated and outside the scope of this work. However, for $H \to \infty$ and T_0 very close to $T_{\rm C}$ it is given by a simple linear expression,

$$\Delta T_{\rm ad} = T_0 + \tfrac{21}{13}(T_0 - T_{\rm C}), \qquad (6)$$

which is an adaptation for Gd of a more general equation (A.6), derived in the appendix. Thus, there should be an abrupt change of slope at $T_0 = T_C$, by a factor of 2.6 for Gd, but no maximum.

Recent years have seen a steady progress in using pulsed magnetic fields in magnetocaloric research[5–10]. Techniques have been developed for direct MCE measurements in fields as high as $\sim 60\,\mathrm{T}$ [5,9,10]. However, despite the earlier predictions[3], the functional relations valid in such strong fields and the experimentally determined quantitative knowledge of the MCE was essentially limited to $\sim 10\,\mathrm{T}$[2]. Here we present a theory-guided, systematic study of gadolinium in pulsed fields of up to 62 T, aimed specifically at the acurate determination of the MCE. This work is organized as follows. First, the experimental techniques and the theory are described. Subsequently, the results are presented, discussed, and compared to theory followed by a concluding assessment.

II. EXPERIMENTAL DETAILS

In order to prepare a single-crystal specimen, polycrystalline gadolinium metal of 99.96 wt.% purity (with respect to all stable elements in the periodic table) prepared by the Materials Preparation Center of Ames Laboratory was cast into a cylinder that was then strained by mechanical impact. The cylinder was suspended inside a sealed tantalum container by a tantalum wire and placed in an electric resistance furnace. It was annealed at $\approx 1200\,^{\circ}\mathrm{C}$ for 24 hours under inert atmosphere[11]. One of the large resulting grains was then oriented to the $\langle 0001 \rangle$ direction by x-ray back-reflection Laue and a 3 mm cylinder was spark cut from the oriented grain. The orientation of the face was refined using Laue technique, and the faces ground parallel on 600 grit SiC paper.

To prepare a spherical sample, a rectangle was cut out with a square cross section that was slightly larger than the diameter of the sphere desired. The rectangle was cut such that the long dimension of the rectangle was parallel to the $\langle 0001 \rangle$ crystallographic direction. The rectangle was made long enough to be chucked in a submersible lathe and was placed in the tank of a sinker electrodischarge machine (EDM). A brass tube of appropriate internal diameter was used as the electrode. As the tube spark cut the rotating crystal, a sphere was formed. The EDM was stopped just before it cut through, first to keep the sphere from being lost in the tank, but secondly so that there were small nubs on the sphere indicating the $\langle 0001 \rangle$ direction. The nubs were filed smooth, after the sample was electro-polished to provide a barrier against oxidation.

The adiabatic temperature change was measured in the Dresden High Magnetic Field Laboratory using a pulsed-field magnet generating fields up to 62 T. Two hemispherical segments were cut out from the single-cystalline gadolinium sphere using a wire saw. Both segments were glued together with two-component silver epoxy placing in between a differential type-T thermocouple. A wire thickness of 25 µm was used to ensure a sufficiently fast response time of the thermocouple[12]. The sample was then mounted on a plastic holder with the field pointing along the $\langle 0001 \rangle$ direction. Both thermocouple junctions where located in the field center of the magnet coil. Therefore, the field sensitivity of the thermocouple (a few Kelvin in 62 T) can be neglected since both thermocouple junctions shift in the same manner and only the temperature difference between them is considered. The high vacuum inside the sample tube and the short duration of the pulse (time to reach the maximum field was 33 ms) assure almost perfect adiabatic conditions. Adiabatic magnetization curves were measured in the same magnet on a fragment with the same shape and aspect ratio as the sample stack used for the ΔT_{ad} measurements with its c axis along the field direction. The magnetization was measured using the induction method and a coaxial pick-up coil system. A detailed description of the pulsed-field magnetometer can be found in Ref.[13]. Isothermal $M(H)$ curves up to 14 T were obtained using a commercial vibrating-sample magnetometer (Quantum Design PPMS-14). These isothermal magnetization data and the pulsed-field ΔT_{ad} results were used to determine grid points for rescaling the adiabatic $M(H)$ results from pulsed-field measurements to absolute values. These were utilized to correct demagnetizing effects. Quasi-static measurements of ΔT_{ad} in fields up to 1.93 T were obtained using a purpose-built device with two nested Halbach magnets as field source. More details about the latter setup can be found elsewhere[14,15].

III. THEORY

In order to visualize the anticipated evolution of $\Delta T_{\mathrm{ad}}(T_0)$, the simple approach outlined in the Introduction needs to be generalized to finite H.

We begin by augmenting Eq. (2) with an extra term,

$$0 = 3Nk_{\mathrm{B}} \ln\left(\frac{T}{T_0}\right) - N_M k_{\mathrm{B}} \ln(2J+1) + S_M. \qquad (7)$$

The added term, S_M, represents the magnetic entropy of the final state, no longer assumed to be saturated. Therefore, S_M is now nonzero. It is given by Eq. (1.22) of Ref.[16]:

$$S_M = N_M k_{\mathrm{B}} \left[\ln \frac{\sinh\left(\frac{2J+1}{2J}x\right)}{\sinh\left(\frac{1}{2J}x\right)} - xB_J(x)\right], \qquad (8)$$

where $B_J(x)$ is the Brillouin function and

$$x = \frac{\mu\mu_0 H + \frac{3J}{J+1}\, k_{\mathrm{B}} T_{\mathrm{C}} B_J(x)}{k_{\mathrm{B}} T}. \qquad (9)$$

This expression is characteristic for the molecular-field theory[16]. The first term in the numerator of Eq. 9 is the energy due to the applied magnetic field, μ being the

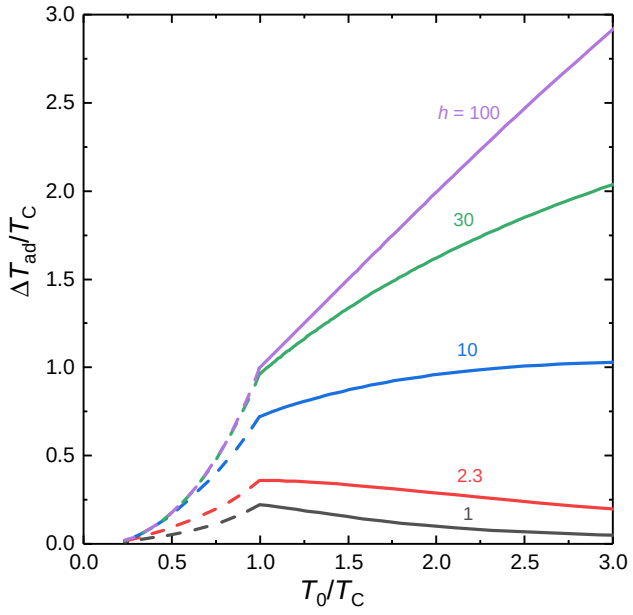

FIG. 1. Calculated reduced adiabatic temperature change of Gd as function of the reduced initial temperature for different values of the dimensionless magnetic field, h, defined in Eq. 12. The dependence for $T_0 < T_C$ (dashed curves) is complex to derive and is not considered in this work.

atomic magnetic moment. The second term desribes the molecular field; it is proportional to the reduced magnetization,

$$\sigma = B_J(x). \tag{10}$$

For simplicity, the following calculations are limited to the special case of Gd: $N_M = N$, $J = 7/2$, $\mu = 7\mu_B$. The final temperature is expressed using Eq. (9):

$$T = T_C \frac{h + \frac{7}{3} B_J(x)}{x}, \tag{11}$$

where h is the dimensionless "magnetic field",

$$h = \frac{7\mu_B \mu_0 H}{k_B T_C}. \tag{12}$$

The combination of Eqs. (7) and (8) is solved for the initial temperature,

$$T_0 = T \left[\frac{\sinh \frac{8}{7}x}{8 \sinh \frac{1}{7}x} \, e^{-xB_J(x)} \right]^{1/3}. \tag{13}$$

It is convenient to eliminate T from this expression by using Eq. (11):

$$T_0 = T_C \frac{h + \frac{7}{3} B_J(x)}{x} \left[\frac{\sinh \frac{8}{7}x}{8 \sinh \frac{1}{7}x} \, e^{-xB_J(x)} \right]^{1/3}. \tag{14}$$

Finally, Eq. (14) is subtracted from Eq. (11) to yield the adiabatic temperature change:

$$\Delta T_{ad} = T_C \frac{h + \frac{7}{3} B_J(x)}{x} \times \left\{ 1 - \left[\frac{\sinh \frac{8}{7}x}{8 \sinh \frac{1}{7}x} \, e^{-xB_J(x)} \right]^{1/3} \right\} \tag{15}$$

The conjunction of Eqs. (14) and (15) provides a parametric representation of the dependence of ΔT_{ad} on T_0, x being the parameter. This dependence is plotted in Fig. 1 (solid lines) for several fixed values of h. ΔT_{ad} increases as a function of T_0 for h large and $T_0 > T_C$. This increase persists up to very high temperature, given by $T_{max} \approx 2.2\, k_B^{-1} \mu_B \mu_0 H \gg T_C$ (not shown in Fig. 1), where $\Delta T_{ad}(T_0)$ exhibits a broad maximum. The dashed lines in the ferromagnetic region ($T_0/T_C < 1$) require more involved self-consistent calculations and are not under discussion herein. Just note that very close to the Curie point the dashed curves can be regarded as approximately linear and described by explicit expressions similar to Eq. (6).

In order to describe the field dependence of ΔT_{ad} at $T_0 = T_C$, T_C is subtracted from Eq. (11), which results in

$$\Delta T_{ad} = T_C \left[\frac{h + \frac{7}{3} B_J(x)}{x} - 1 \right]. \tag{16}$$

Then Eq. (14), with $T_0 = T_C$, is solved for h:

$$h = x \left[\frac{8 \sinh \frac{1}{7}x}{\sinh \frac{8}{7}x} \, e^{xB_J(x)} \right]^{1/3} - \frac{7}{3} B_J(x). \tag{17}$$

The combination of Eqs. (16) and (17) provides a parametric representation of the dependence of ΔT_{ad} on h (or on H). For x and h small, $h \approx \frac{47}{294} x^3$ and

$$\frac{\Delta T_{ad}}{T_C} \approx \frac{1}{14} x^2 \approx \frac{1}{14} \left(\frac{294}{47} \right)^{2/3} h^{2/3}. \tag{18}$$

This is the well-known $H^{2/3}$ power law derived by Oesterreicher & Parker[17]. When h increases, it proves useful to include the next term in the expansion,

$$\frac{\Delta T_{ad}}{T_C} = \frac{1}{14} \left(\frac{294}{47} \right)^{2/3} h^{2/3} - \frac{21,451}{13,541,640} \left(\frac{294}{47} \right)^{4/3} h^{4/3} = 0.242\, h^{2/3} - 0.018\, h^{4/3}. \tag{19}$$

This expression is accurate to 1% for $h \leq 1$ (which corresponds to $\mu_0 H \leq 62$ T).

IV. RESULTS AND DISCUSSION

Figure 2 presents the results of direct measurements of the adiabatic temperature change as a function of applied

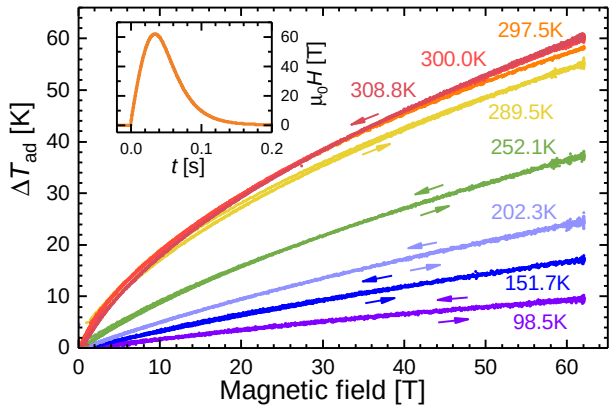

FIG. 2. Adiabatic temperature change ΔT_{ad} of a gadolinium single crystal in pulsed magnetic fields up to 62 T at different initial temperatures T_0. For all curves, both the magnetization and the demagnetization branches are plotted. Experimental data presented in this and other figures are measured with the magnetic field vector along the $\langle 0001 \rangle$ direction. The inset shows the temporal profile of the magnetic field pulse. The rise time amounts to 33 ms.

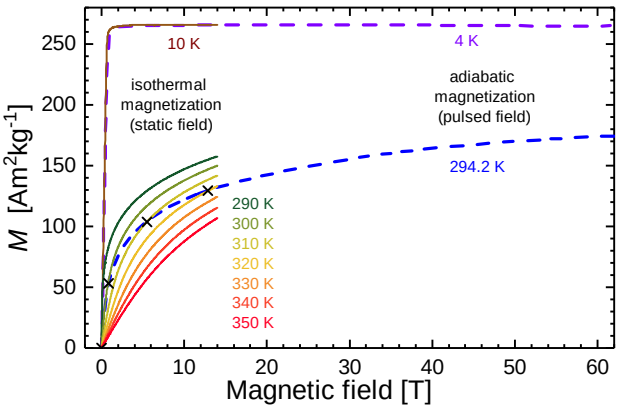

FIG. 4. Magnetization as a function of applied magnetic field. The solid lines represent isothermal measurements up to 14 T and the dashed curves were obtained in adiabatic pulsed-field experiments. Due to the large temperature increase during the pulse, the adiabatic curve strongly deviates from the isothermal results. Considering the adiabatic temperature changes in Fig. 2, it is possible to determine grid points (crosses) in order to match the pulsed-field data to the isothermally determined values of the magnetization.

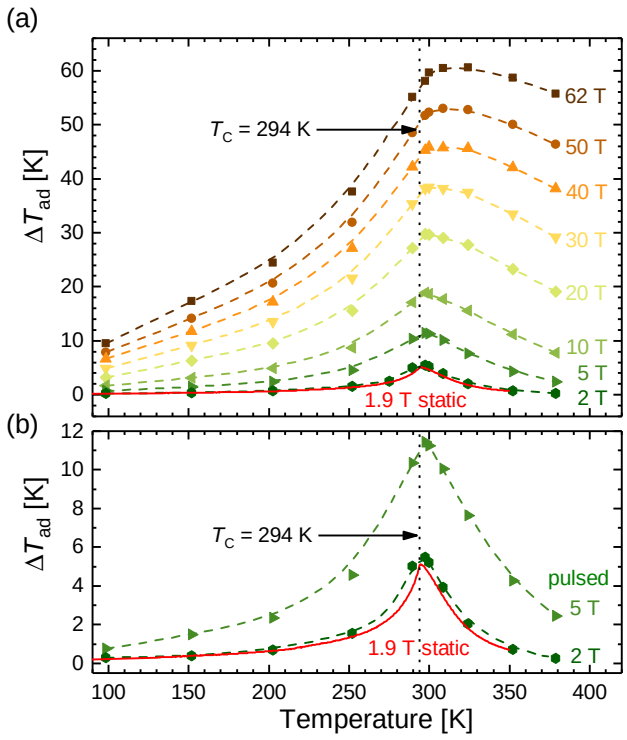

FIG. 3. (a) Adiabatic temperature change ΔT_{ad} as a function of temperature for different magnetic fields. The data points were extracted from the magnetic-field dependences of ΔT_{ad} for given field values. They are connected with dashed lines as a guide to the eye. The solid line shows the data obtained from direct measurements of the adiabatic temperature change under quasi-static conditions. (b) shows the low-field region of (a).

magnetic field, for several starting temperatures T_0. The maximum MCE measured was 60.5 K in a field of 62 T, for T_0 just above 300 K. Even when the starting temperature is far below the Curie temperature, at $T_0 = 100$ K, ΔT_{ad} in 62 T is as high as 10 K, scaling almost linearly with the field. Closer to T_{C}, the field dependence of ΔT_{ad} has a noticeable negative curvature that flattens out towards higher fields.

The inset of Fig. 2 shows the typical shape of a field pulse. One can appreciate that the rise time is about 33 ms and the fall time is three times longer. For all curves in Fig. 2 both the magnetization and demagnetization branches are plotted. No significant hysteresis can be observed, which is evidence of the high quality of our measurements and sufficiently short response time of the thermocouple. It is also clear that no appreciable eddy-current heating took place. Indeed, eddy currents induced by the changing magnetic field would have additionally heated up the sample, both on rising and falling field; as a result, the temperature after the pulse would have been higher than the starting temperature, T_0. Yet, in the present experiments, as well as in our previous studies[9,12], the temperature always returned to its initial value, T_0, as soon as the pulse was over.

A number of points were selected from the data array shown in Fig. 2, these points were arranged in several series according to the value of the applied magnetic field and plotted against starting temperature, T_0, as shown in Fig. 3. The vertical dotted line marks the Curie temperature, $T_{\mathrm{C}} = 294$ K. In low fields (< 10 T, Fig. 3b) the $\Delta T_{\mathrm{ad}}(T_0)$ dependence is caret-shaped and approximately symmetric, the maximum being at $T_0 = T_{\mathrm{C}}$;

this is in agreement with direct $\Delta T_{\rm ad}$ measurements in a static field of 1.9 T (solid line in Fig. 3). In very strong magnetic fields, the shape of the $\Delta T_{\rm ad}(T_0)$ dependence is clearly asymmetric – the low-temperature slope is steeper than the high-temperature one – the maximum is broader and situated distinctly above $T_{\rm C}$. The observed shift of the maximum is an extrinsic effect caused by the asymmetry of the peak and its smearing out due to imperfect homogeneity of the sample. The true, intrinsic departure of the maximum from $T_{\rm C}$ towards much higher temperatures is only expected to take place in fields of more than 140 T, which corresponds to $h = 2.3$ in Figure 1. Of particular interest is the emergence of a broad temperature range where the magnetocaloric effect is large and nearly constant. Taking for example the 62 T curve, the interval where $\Delta T_{\rm ad} \approx 60$ K extends from 300 to 350 K. The theoretical predictions summarized in Fig. 1 suggest that this interval should become yet much wider in higher magnetic fields.

The use of high pulsed magnetic fields to study the MCE of gadolinium was pioneered by Ponomarev[18]. The maximum field available in Ref.[18] was as high as 35 T, yet $\Delta T_{\rm ad}$ was determined indirectly from measured adiabatic magnetization. As regards direct MCE measurements, we are aware of just one previous work where $\Delta T_{\rm ad}$ of Gd metal was measured in comparable magnetic fields[19]. The maximum temperature change was $\Delta T_{\rm ad} = 60$ K, for the strongest available field of 55 T and $T_0 = 295$ K. Our value for 55 T and $T_0 = 294.9$ K is $\Delta T_{\rm ad} = 54$ K, that is 10 % less. The discrepancy cannot be explained by the difference in the sample quality. In Ref.[19] the measurements were performed on commercial polycrystalline Gd containing 12 times more impurities than our starting material. If anything, our $\Delta T_{\rm ad}$ should have been higher. The overestimation of the MCE in Ref.[19] is probably related to the neglect of magnetostriction of gadolinium. The temperature in Ref.[19] was determined from measurements of the electrical resistance of a thin layer of gold deposited on the Gd sample and field-induced strain (magnetostriction) was ignored when calibrating the thermometer in Ref.[19]. We employ thin thermocouples, which are insensitive to strain.

Since the experimental results of Ref.[19] are claimed to be in agreement with the molecular-field calculations, we decided to carry out a similar comparison of our own results with theoretical predictions. For the comparison, the measured $\Delta T_{\rm ad}(H)$ curves had to be corrected for demagnetization. To this end, magnetization measurements were performed in the same pulsed-field coil as the one employed in the $\Delta T_{\rm ad}$ experiments, on a specially cut single crystal having the same aspect ratio and orientation as the aggregate sample used to measure $\Delta T_{\rm ad}$. Magnetization was also measured in isothermal conditions, in quasi-static magnetic fields, on the same single crystal. The isothermal and selected adiabatic magnetization curves are displayed in Fig. 4 as solid and dashed lines, respectively. At low temperatures ($T = 4$ and 10 K) the curves of both kinds lie close together. The

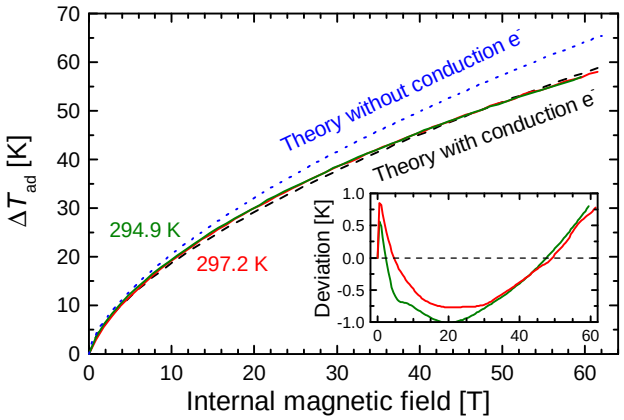

FIG. 5. Comparison of the adiabatic temperature change at two different starting temperatures near $T_{\rm C}$ and the theoretical curve with and without contribution of the conduction electrons to the heat capacity (dashed and dotted curve). The inset shows the difference between the theoretical and the experimental curves.

initial slope of the low-temperature isotherms yielded $N = 2.6 \times 10^{-3}$ for the demagnetizing factor. At elevated temperatures the magnetocaloric effect is strong and the two kinds of curves differ considerably. Namely, the displayed adiabate intersects the isotherms, taken at regular intervals of 10 K. The crossing-points marked in the diagram were used to scale the pulsed-field magnetization to absolute values, the evolution of temperature along the adiabate being known from the previous $\Delta T_{\rm ad}$ measurements.

Finally, the magnetic field in selected $\Delta T_{\rm ad}(H)$ data sets was corrected by using the adiabatic $M(H)$ curves with possibly close values of T_0 and the standard expression, $H_{\rm int} = H - NM(H)$. Two of the corrected curves, with T_0 just above $T_{\rm C}$, are shown in Fig. 5. The theoretical dependence, given by Eq. 19 and shown by dotted line in Fig. 5, overestimates $\Delta T_{\rm ad}$ by as much as 13 %. The overestimation can be attributed to the neglect of the contribution of conduction electrons to the specific heat of Gd. The model proposed in Ref.[3] and adopted in Section III is rather general and applies to all rare earth compounds. The generality has its price, particularly, when it comes to metals, since conduction electrons are simply neglected in the model. Let us now include their contribution to the specific heat. According to Brown, [20] $\gamma = 2.6 \times 10^{-3}$ cal mol^{-1} K^{-1}, or 1.3×10^{-3} R/K. This yields $\gamma T \approx 0.42$ R at $T \approx 320$ K; the weak dependence on T will henceforth be neglected. Consequently, the total non-magnetic specific heat (lattice + conduction electrons) is 3.42 R rather than $3R$. Therefore, the equations of Section III should be modified as follows.

(i) The prefactor $3k_{\rm B}N$ in the first term of Eq. (7) should be replaced by 3.42 $k_{\rm B}N$.

(ii) The exponent of the square brackets in Eqs. (13-15)

should be 1/3.42 rather than 1/3.

(iii) The coefficients of the expansion (19) should become

$$\frac{3}{14\times 3.42}\left(\frac{3}{14\times 3.42}+\frac{13}{147}\right)^{-2/3}$$

and

$$\frac{46,305-26,596\times 3.42^2}{96,040\times 3.42^2\times(63+26\times 3.42)}\left(\frac{3}{14\times 3.42}+\frac{13}{147}\right)^{-4/3}$$

As a result, the modified expansion (19) should read

$$\frac{\Delta T_{\rm ad}}{T_{\rm C}} = 0.221\,h^{2/3} - 0.019\,h^{4/3}. \qquad (20)$$

This expression, with $T_{\rm C} = 294\,{\rm K}$ and h as defined by Eq. (12), was used to produce the solid curve shown in Fig. 5. Agreement with the experiment is quite satisfactory this time (the difference between theory and experiment is shown in the inset of Fig. 5). Given that our model contains no adjustable parameters and that the calculations leading to Eq. (20) were carried out by hand, we are reasonably confident that the dashed curve in Fig. 5 presents the true molecular-field result and that the calculations of Ref.[19], performed numerically, with no details reported, went wrong at some stage. The disagreement cannot be accounted for by the model, which is much the same in this work and in Ref.[19]. Their background specific heat was somewhat too high, $30\,{\rm J\,mol^{-1}\,K^{-1}}$ or $3.6R$ (as against $3.42R$ in our work), which should have resulted in an underestimation of $\Delta T_{\rm ad}$. Yet, the calculated $\Delta T_{\rm ad}(H)$ curve of Ref.[19] lies about 13 % too high; incidentally, it is very close to the dotted curve in our Fig. 5 (calculated with a background of $3R$). So, there must be a numerical error in the calculations of Ref.[19]. Be it as it may, our calculations do agree with our experimental data and disagree with those of Ref.[19].

V. CONCLUSIONS

Direct measurements of the magnetocaloric effect in Gd have been carried out in pulsed magnetic fields of up to 62 T, at which point a very large adiabatic temperature change of 60.5 K has been observed. The magnetic field dependence of $\Delta T_{\rm ad}$ is found to follow the familiar molecular-field expression with a leading term in $H^{2/3}$ and a correction term in $H^{4/3}$. However, regarded as a function of starting temperature, $\Delta T_{\rm ad}(T_0)$ at H = const., it shows a number of features not observed previously. Thus, the sharp and symmetric (caret-shaped) maximum at the Curie point becomes broad and asymmetric; its high-temperature slope becomes less steep and tends to develop into a wide plateau stretching from $T_{\rm C}$ upwards. Calculations predict that in yet higher fields (140 T) the maximum at $T_0 = T_{\rm C}$ should turn into a simple kink and that $\Delta T_{\rm ad}(T_0)$ should grow up until a new, very broad maximum situated far above $T_{\rm C}$.

ACKNOWLEDGMENTS

This work was supported by DFG (Grant No. SPP 1599) and by HLD at HZDR, member of the European Magnetic Field Laboratory (EMFL). We acknowledge the Helmholtz Association for funding via the Helmholtz-RSF Joint Research Group (Project No. HRSF-0045). The Ames Laboratory is operated for the U. S. Department of Energy by Iowa State University of Science and Technology under contract No. DE-AC02-07CH11358 and is supported by the Office of Basic Energy Sciences, Materials Sciences and Engineering Division.

* t.gottschall@hzdr.de

[1] K. A. Gschneidner and V. K. Pecharsky, Ann. Rev. Mater. Sci. **30**, 387 (2000).
[2] A. Tishin and Y. Spichkin, *The Magnetocaloric Effect and Its Applications* (Institute of Physics, 2003) pp. 69 – 95.
[3] V. Druzhinin, V. Mel'nikov, and V. Shkarubskii, Sov. Phys. Solid State **21**, 1002 (1979).
[4] M. Rosen, Phys. Rev. **174**, 504 (1968).
[5] T. Kihara, X. Xu, W. Ito, R. Kainuma, and M. Tokunaga, Phys. Rev. B **90**, 214409 (2014).
[6] C. Salazar Mejía, M. Ghorbani Zavareh, A. K. Nayak, Y. Skourski, J. Wosnitza, C. Felser, and M. Nicklas, J. Appl. Phys. **117**, 17E710 (2015).
[7] M. Ghorbani Zavareh, C. Salazar Mejía, A. K. Nayak, Y. Skourski, J. Wosnitza, C. Felser, and M. Nicklas, Appl. Phys. Lett. **106**, 071904 (2015).
[8] M. Fries, T. Gottschall, F. Scheibel, L. Pfeuffer, K. Skokov, I. Skourski, M. Acet, M. Farle, J. Wosnitza, and O. Gutfleisch, J. Magn. Magn. Mater. **477**, 287 (2019).
[9] F. Scheibel, T. Gottschall, K. Skokov, O. Gutfleisch, M. Ghorbani-Zavareh, Y. Skourski, J. Wosnitza, O. Cakir, M. Farle, and M. Acet, J. Appl. Phys. **117**, 233902 (2015).
[10] M. G. Zavareh, Y. Skourski, K. P. Skokov, D. Y. Karpenkov, L. Zvyagina, A. Waske, D. Haskel, M. Zhernenkov, J. Wosnitza, and O. Gutfleisch, Phys. Rev. Appl. **8**, 014037 (2017).
[11] B. Beaudry and K. Gschneidner, in *Metals*, Handbook on the Physics and Chemistry of Rare Earths, Vol. 1 (Elsevier, 1978) pp. 173 – 232.

[12] T. Gottschall, K. P. Skokov, F. Scheibel, M. Acet, M. G. Zavareh, Y. Skourski, J. Wosnitza, M. Farle, and O. Gutfleisch, Phys. Rev. Applied **5**, 024013 (2016).
[13] Y. Skourski, M. D. Kuz'min, K. P. Skokov, A. V. Andreev, and J. Wosnitza, Phys. Rev. B **83**, 214420 (2011).
[14] J. Liu, T. Gottschall, K. P. Skokov, J. D. Moore, and O. Gutfleisch, Nat. Mater. **11**, 620 (2012).
[15] O. Gutfleisch, T. Gottschall, M. Fries, D. Benke, I. Radulov, K. P. Skokov, H. Wende, M. Gruner, M. Acet, P. Entel, and M. Farle, Phil. Trans. R. Soc. A **374**, 20150308 (2016).
[16] J. S. Smart, *Effective Field Theories of Magnetism* (Philadelphia: Saunders, 1966).
[17] H. Oesterreicher and F. Parker, J. Appl. Phys. **55**, 4334 (1984).
[18] B. Ponomarev, J. Magn. Magn. Mater. **61**, 129 (1986).
[19] T. Kihara, Y. Kohama, Y. Hashimoto, S. Katsumoto, and M. Tokunaga, Rev. Sci. Instrum. **84**, 074901 (2013).
[20] G. V. Brown, J. Appl. Phys. **47**, 3673 (1976).

Appendix: DERIVATION OF Eq. (6)

Like in the Introduction, in the final state ($H = \infty$) the system is magnetized to saturation and has $S_M = 0$. The difference is in the initial state ($H = 0$): now it is not fully demagnetized, there is a small spontaneous magnetization σ. Just below the Curie point the square of the spontaneous magnetization varies linearly with temperature, cf. Eq. (3.26) of Ref.[16]:

$$\sigma^2 = \frac{10}{3}\,\frac{(J+1)^2}{(J+1)^2+J^2}\,\frac{T_\mathrm{C}-T_0}{T_\mathrm{C}}. \tag{A.1}$$

At the same time, Eq. (10) turns into a simple proportionality relation between σ and x:

$$\sigma = \frac{J+1}{3J}\,x. \tag{A.2}$$

In Eqs. (A.1) and (A.2) x, σ, and $(T_\mathrm{C}-T_0)/T_\mathrm{C}$ must be small as compared with unity. Under the same conditions, Eq. (8) becomes

$$S_M = N_M k\left[\ln(2J+1) - \frac{J+1}{6J}\,x^2\right]. \tag{A.3}$$

Here the first term in brackets decribes the fully demagnetized initial state considered in the Introduction, while the second term is a correction for small initial magnetization. Note that Eq. (1.37) in Smart's book[16], which corresponds to our Eq. (A.3), has a misprint: the denominator of the second term there equals $3J$, rather than $6J$. Now, eliminating x by means of Eqs. (A.1) and (A.2), one has

$$S_M = N_M k\left[\ln(2J+1) - \frac{5J(J+1)}{2J^2+2J+1}\,\frac{T_\mathrm{C}-T_0}{T_\mathrm{C}}\right] \tag{A.4}$$

The negative of this expression is to replace the second term in Eq. (2), which is then solved for T by iterations, making use of the smallness of $(T_\mathrm{C}-T_0)/T_\mathrm{C}$. The result is

$$\begin{aligned} T = {} & (2J+1)^{N_M/3N}T_0 \\ & + \frac{N_M}{3N}\,\frac{5J(J+1)(2J+1)^{N_M/3N}}{2J^2+2J+1}\,(T_0-T_\mathrm{C}). \end{aligned} \tag{A.5}$$

Hence,

$$\begin{aligned} \Delta T_\mathrm{ad} = {} & \left[(2J+1)^{N_M/3N}-1\right]T_0 \\ & + \frac{N_M}{3N}\,\frac{5J(J+1)(2J+1)^{N_M/3N}}{2J^2+2J+1}\,(T_0-T_\mathrm{C}). \end{aligned} \tag{A.6}$$

This leads to Eq. (6) for Gd, with $N_M = N$ and $J = 7/2$.